Discover Chemical Engineering

Discover

Perspective

Thermodynamic and kinetic considerations of nitrogen carriers for chemical looping ammonia synthesis

Wenbo Gao[1,2] · Runze Wang[1,2] · Sheng Feng[1,3] · Yawei Wang[1,2] · Zhaolong Sun[1,2] · Jianping Guo[1,2] · Ping Chen[1,2]

Received: 15 November 2022 / Accepted: 9 January 2023
Published online: 14 January 2023

Abstract
Ammonia (NH_3) is a promising clean energy carrier, provided that its production is driven by renewable energy rather than fossil fuel-based Haber–Bosch (H–B) process. Chemical looping ammonia synthesis (denoted as CLAS) can intervene in the ubiquitous scaling relations in catalytic ammonia synthesis by separately feeding reactants to a nitrogen carrier to achieve atmospheric operation, which provides an alternative synthetic route to the H-B process. The key of CLAS is to develop efficient N carrier materials with suitable thermodynamic and kinetic properties. Metal nitrides and metal imides are two kinds of N carrier materials for the CLAS process, and H_2 and H_2O are commonly used as the hydrogen sources of NH_3. Here, we first analyze the thermodynamic properties of the reactions of various metal nitrides and imides with water or hydrogen to produce NH_3, N_2 fixation on metals or metal hydrides, and the regeneration of metals from metal oxides, respectively. The thermodynamic calculation results display the reduction of main group metal hydroxide, early transition metal oxides, and rare earth metal oxides to the corresponding metallic state or hydrides, the nitridation of late transition metals to the corresponding nitrides, are the thermodynamic limiting steps for the metal nitride carriers. The metal imides, such as lithium imide and barium imide, have the relatively proper thermodynamics for two-step chemical looping reactions, however, their performance is limited by the thermodynamics of hydrogenation reaction. Moreover, for the thermodynamically unfavorable steps in the CLAS, we propose potential electrochemical processes to run the loop, such as molten salt electrolytic cell and solid electrolyte electrolytic cell. Finally, we put forward some strategies, such as controllable synthesis of N carriers and adding efficient catalysts, to improve the kinetics of chemical looping reactions.

1 Introduction

Ammonia, with the advantages of high hydrogen content (17.8 wt.%), high energy density (22.5 MJ/kg), facile storage and transportation, etc., has been considered a promising energy vector in recent years [1–3]. However, the industrial ammonia synthesis based on the Haber–Bosch (H–B) process requires harsh reaction conditions (150–250 bar and 400–500 °C) consuming more than 1% of the global energy supply and accounting for about 1.2% of global CO_2 emissions [3–5]. Besides, ammonia decomposition to produce CO_x-free hydrogen is another important aspect to achieve the utilization of

Supplementary Information The online version contains supplementary material available at https://doi.org/10.1007/s43938-023-00019-4.

✉ Wenbo Gao, gaowenbo@dicp.ac.cn | [1]Dalian Institute of Chemical Physics, Chinese Academy of Sciences, Dalian 116023, China. [2]University of Chinese Academy of Sciences, Beijing 100049, China. [3]Zhang Dayu School of Chemistry, Dalian University of Technology, Dalian 116024, China.

ammonia energy. Therefore, the development of alternative and sustainable ammonia production and ammonia decomposition processes is highly in demand. Encouraging progress has been made in catalytic and chemical looping ammonia synthesis (CLAS) as well as ammonia decomposition processes driven by thermal, electrical, or light energies [2, 6–13].

CLAS decouples ammonia synthesis reaction into multiple sub-reactions mediated by an intermediate N carrier material. Compared to the conventional catalytic ammonia synthesis process where the reactants (i.e., the N_2+H_2 mixture) are co-fed into the reactor, the CLAS process is carried out by separately feeding N_2 and H_2 (or H_2O) under the same or different reaction conditions as shown in Fig. 1. This process has the following merits: (i) avoiding the competitive adsorption between N_2 and H_2 (or H_2O); (ii) regulating the thermodynamic and kinetic properties of each sub-reaction by designing suitable N carrier materials and choosing optimized reaction conditions. Thereby, the CLAS can address to certain degree the dilemma of efficient dinitrogen activation requiring high temperature and high equilibrium yield of NH_3 at lower temperature [14].

There have been several reviews on CLAS [2, 6, 15–17]. A recent review by Fan and Liu et al. provided a comprehensive summarization of previous CLAS processes and discussed the assistance of plasma technology and artificial intelligence in CLAS [6]. Bollas et al. carried on systematic analysis on thermodynamic feasibility from the point of technical process in terms of energy consumption, process footprint, and initial cost. [18]. Several other papers had assessed technological feasibility and applicability and analyzed the system integration and exergy cost of CLAS process [19–21]. However, there is a lack of the systematically thermodynamic and kinetic considerations over various N carriers for CLAS. This article aims to offer a perspective on thermodynamic and kinetic improvement of the nitrides and imides materials in the CLAS processes, typically the thermodynamic and kinetic consideration of the electricity-driven CLAS was analyzed.

2 The development of N carriers in CLAS

The N carrier materials are crucial to the CLAS process. Table 1 summarizes various N carrier materials reported in literature and lists related information including hydrogen sources, chemical loops, and sub-reactions. Metal nitrides (denoted as MNs) and metal imides (denoted as MNHs) are types of N carriers under investigations. On the other hand, according to the hydrogen sources, the CLAS processes can be divided into two categories: (1) H_2-CLAS where H_2 is the H source and (2) H_2O-CLAS where H_2O is used as the H source. The history of CLAS can be traced back to the nineteenth century when Tessie du Motay proposed ammonia synthesis via a two-step cycle between TiN (or Ti_3N_2) and Ti_5N_3 through H_2-CLAS [22]. Then, Haber studied ammonia synthesis over Mn_3N_2-Mn and Ca_3N_2-CaH_2 cycles, which is a prelude to the development of the H-B process [23]. It is worthy of noting that an ammonia production loop mediated by calcium cyanamide

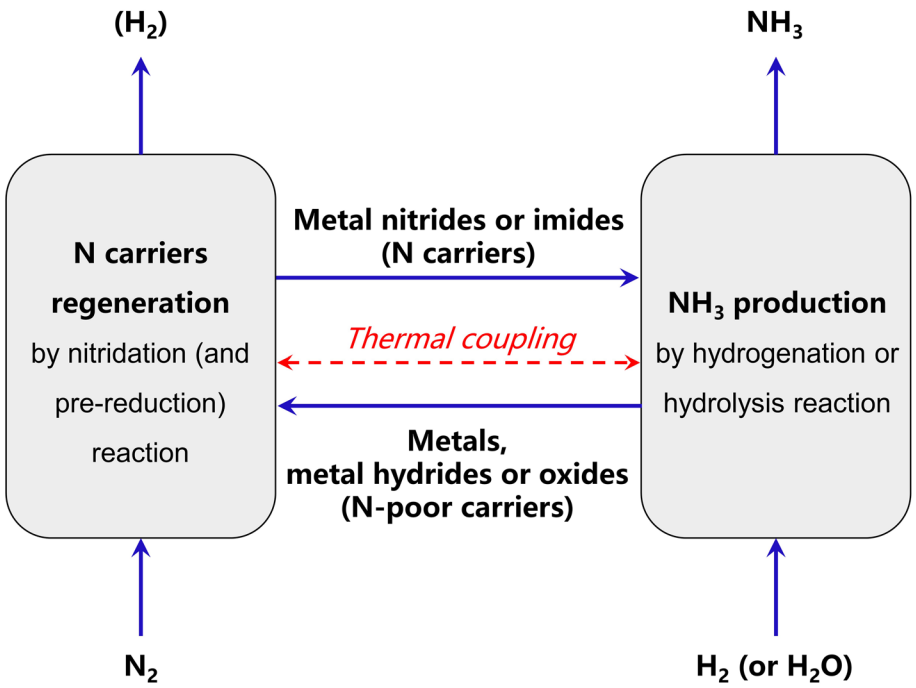

Fig. 1 Schematic diagrams of chemical looping ammonia synthesis

Table 1 Chemical looping reactions over various N carriers

Types of CLAS	Types of N carriers	Chemical loops	Sub-reactions	Refs.
H_2O-CLAS	Cyanamides	$CaCN_2$-$CaCO_3$-CaC_2	N_2 fixation: $CaC_2 + N_2 \rightarrow CaCN_2 + C$ NH_3 production: $CaCN_2 + 3H_2O \rightarrow 2NH_3 + CaCO_3$ Regeneration: $CaCO_3 + 5/2C \rightarrow CaC_2 + 3/2CO_2$	[24]
	Nitrides	AlN-Al_2O_3	N_2 fixation: $Al_2O_3 + 3C + N_2 \rightarrow 2AlN + 3CO$ or $Al_2O_3 + 3CH_4 + N_2 \rightarrow 2AlN + 6H_2 + 3CO$ NH_3 production: $2AlN + 3H_2O \rightarrow Al_2O_3 + 2NH_3$	[27]
		Cr_2N-Cr_2O_3-Cr	N_2 fixation: $2Cr + 1/2N_2 \rightarrow Cr_2N$ NH_3 production: $Cr_2N + 3H_2O \rightarrow Cr_2O_3 + NH_3 + 3/2H_2$ Regeneration: $Cr_2O_3 + 3H_2 \rightarrow 2Cr + 3H_2O$ or $Cr_2O_3 + 3CO \rightarrow 2Cr + 3CO_2$	[44]
		Mo_2N-MoO_2-Mo	N_2 fixation: $2Mo + 1/2N_2 \rightarrow Mo_2N$ NH_3 production: $Mo_2N + 4H_2O \rightarrow 2MoO_2 + NH_3 + 5/2H_2$ Regeneration: $MoO_2 + 2H_2 \rightarrow Mo + 2H_2O$ or $2MoO_2 + 4CO \rightarrow 2Mo + 4CO_2$	[49]
		Mn_5N_2-MnO-Mn	N_2 fixation: $5/2Mn + 1/2N_2 \rightarrow 1/2Mn_5N_2$ NH_3 production: $1/2Mn_5N_2 + 5/2H_2O \rightarrow 5/2MnO + NH_3 + H_2$ Regeneration: $MnO + H_2 \rightarrow Mn + H_2O$	[50]
		Li_3N-LiOH-Li	N_2 fixation: $6Li + N_2 \rightarrow 2Li_3N$ NH_3 production: $2Li_3N + 6H_2O \rightarrow 6LiOH + 2NH_3$ Regeneration: $6LiOH \xrightarrow{\text{electrolyze}} 6Li + 3H_2O + 3/2O_2$	[31]
		Mg_3N_2-MgO-Mg	N_2 fixation: $3\ Mg + N_2 \rightarrow Mg_3N_2$ NH_3 production: $Mg_3N_2 + 3H_2O \rightarrow 3MgO + 2NH_3$ Regeneration: $MgO + CH4 \xrightarrow{h\nu} Mg + 2H_2 + CO$	[32]
H_2-CLAS	Nitrides	TiN-Ti_5N_3 or Ti_3N_2-Ti_5N_3	N_2 fixation: $TiN_x + (y\text{-}x)/2N_2 \rightarrow TiN_y$ NH_3 production: $TiN_y + 3(y\text{-}x)/2H_2 \rightarrow TiN_x + (y\text{-}x)NH_3$	[22]
		Mn_3N_2-Mn	N_2 fixation: $3Mn + N_2 \rightarrow Mn_3N_2$ NH_3 production: $Mn_3N_2 + 3H_2 \rightarrow 3Mn + 2NH_3$	[23]
		Ca_3N_2-CaH_2	N_2 fixation: $3CaH_2 + N_2 \rightarrow Ca_3N_2 + 3H_2$ NH_3 production: $Ca_3N_2 + 6H_2 \rightarrow 3CaH_2 + 2NH_3$	[23]
		Co_3Mo_3N-Co_6Mo_6N	N_2 fixation: $2Co_6Mo_6N + N_2 \rightarrow 4Co_3Mo_3N$ NH_3 production: $4Co_3Mo_3N + 3H_2 \rightarrow 2Co_6Mo_6N + 2NH_3$	[28]
		$Mn_6N_{2.58}$-Mn_4N	N_2 fixation: $3Mn_4N + 1.08N_2 \rightarrow 2Mn_6N_{2.58}$ NH_3 production: $2Mn_6N_{2.58} + 3.24H_2 \rightarrow 3Mn_4N + 2.16NH_3$	[30]
		Ca_3N_2-Ca_2NH	N_2 fixation: $6Ca_2NH + N_2 \rightarrow 4Ca_3N_2 + 3H_2$ NH_3 production: $2Ca_3N_2 + 3H_2 \rightarrow 3Ca_2NH + NH_3$	[30]
		Sr_2N-SrH_2	N_2 fixation: $4SrH_2 + N_2 \rightarrow 2Sr_2N + 4H_2$ NH_3 production: $2Sr_2N + 7H_2 \rightarrow 4SrH_2 + 2NH_3$	[30]
		Li_3N-Li alloy-LiH	N_2 fixation: $Li_xM + N_2 \rightarrow Li_yM + Li_3N$ NH_3 production: $Li_yM + Li_3N + H_2 \rightarrow Li_zM + LiH + NH_3$ Regeneration: $Li_yM + Li_zM + LiH \rightarrow Li_xM + H_2$ Note: these equations are not balanced	[35]
	Imides	Li_2NH-LiH $BaNH$-BaH_2 $MgNH$-MgH_2 $CaNH$-CaH_2	N_2 fixation: $4AH_x + xN_2 \rightarrow 2xA_{2/x}NH + xH_2$ NH_3 production: $xA_{2/x}NH + 2xH_2 \rightarrow 2AH_x + xNH_3$ (x: valence of A)	[34]
	Imides-Nitrides	Mn_2N/Li_2NH-Mn_4N/LiH Mn_2N/BaNH-Mn_4N/BaH_2	N_2 fixation: $AH_x + yMn_4N + (x/4 + y/2)$ $N_2 \rightarrow x/2A_{2/x}NH + 2yMn_2N + x/4H_2$ NH_3 production: $x/2A_{2/x}NH + 2yMn_2N + (x + 3y/2)$ $H_2 \rightarrow AH_x + yMn_4N + (x/2 + y)NH_3$ (x: valence of A; y: the ratio of Mn_4N and AH_x)	[51]

($CaCN_2$) (Frank-Caro process) was commercialized in 1908 but subsequently was displaced by a more energy-efficient H-B process [24]. In recent ten years, the CLAS attracts the attention of scientists again because of the requirement for building renewable energy-driven ammonia synthesis to replace the current fossil energy-driven H-B process [25, 26]. For instance, Steinfeld et al. designed an H_2O-CALS process mediated by AlN-Al_2O_3 and proposed solar thermal concentrating

for energy supply in 2007 [27]. Hargreaves et al. investigated an H_2-CLAS process mediated by Co_3Mo_3N-Co_6Mo_6N [28]. Pfromm and Michalsky et al. proposed an H_2O-CALS process mediated by Cr_2N-Cr_2O_3-Cr [29], and several H_2-CLAS processes mediated by $Mn_6N_{2.58}$-Mn_4N, Ca_3N_2-Ca_2NH, and Sr_2N-SrH_2, respectively [30]. In general, all of the above H_2O-CLAS processes require extremely high temperatures (≥ 1000 °C), and H_2-CALS proposals have yet been fully implemented experimentally. Recently, some electricity, light or microwave energy-driven CLAS processes were proposed, which have an advantage in breaking the thermal equilibrium limits. Nørskov and Jaramillo et al. designed an electrochemical H_2O-CLAS mediated by Li_3N-LiOH-Li, which was carried out at 400 °C and the potential of ≥ 4.0 V [31]. Halas et al. reported a light-driven H_2O-CLAS process mediated by Mg_3N_2/MgO/Mg [32]. Hu et al. studied the microwave-heated H_2-CLAS over Fe_4N and Co_3Mo_3N [33]. Moreover, Chen and Guo et al. proposed an H_2-CLAS process mediated by alkali or alkaline earth metal hydrides and imides, e.g., Li_2NH/LiH and BaNH/BaH_2, which achieve ammonia synthesis at the atmospheric pressure and lower temperatures (< 300 °C) [34]. Miyaoka et al. systematically studied the dinitrogen dissociation by lithium-group 14 element (Li_xM) alloys, and proposed an H_2-CLAS mediated by Li_xM alloy-Li_3N-LiH [35, 36]. Guan et al. added molten LiCl–KCl in this system and proposed a liquid alloy-molten salt-mediated H_2-CLAS process [37].

The chemical properties of N carriers have great influences on their performances of CLAS. Nitrogen in MNs usually has a formal oxidation state of − 3 as a nitride ion (N^{3-}), and their chemical properties vary greatly with the valence electrons of the metal [18, 38–40]. According to the difference of valence electrons, MNs can be classified as the nitrides of the s-block elements (s-MNs), nitrides of the p-block elements (p-MNs), transition metal nitrides (TMNs), and nitrides of the rare earth elements (RENs), etc. On the other hand, metal imides mainly exist in alkali and alkaline earth metal compounds, rare earth metal compounds, and ternary alkali (or alkaline earth)-transition metal compounds, etc. s-MNHs are of importance for applications in the field of hydrogen storage [41–43]. The reaction thermodynamics of MNs and MNHs reacting with H_2O or H_2 to produce NH_3 as well as the regeneration of MNs and MNHs are the important criteria for their potential applications in the CLAS [27, 30, 34, 44]. In the Sect. 3, we summarized and analyzed the thermodynamics of these reactions according to the type of N carriers and hope to help guiding for the selection of N carriers and the design of the new CLAS processes.

Some sub-reactions in CLAS processes are limited by their reaction thermodynamics, which results in difficulty in closing the chemical loops. For example, the reduction of Al_2O_3 or Cr_2O_3 to the corresponding metal acquires extremely high temperature (above 1000 °C) [27, 44]. It is well-known that extrinsic stimuli (photo, electricity, plasma, and so on) could change the chemical equilibrium of a reaction and thus make the reaction occur under milder conditions [45, 46]. In the industry, the production of metallic Li, Na, K, Al, etc. are carried out under electrolytic conditions because the reduction of their oxides to metals is difficult under normal thermal conditions [47]. Inspired by this, we propose several electrochemical CLAS processes in this perspective. On the other hand, the kinetics of sub-reactions are also crucial to the NH_3 production performances in a CLAS process. For example, the hydrolysis of AlN to produce NH_3 is thermodynamically feasible but is limited by the slow kinetics [48]. In the Sect. 5, we will also discuss some strategies to improve the kinetic properties of N carriers.

3 The reaction thermodynamics of metal nitrides and imides

The N carriers mainly include metal nitrides and imides. In a CLAS process, ammonia can be produced by hydrolysis or hydrogenation of N-rich nitrides or imides accompanied by the formation of oxides, hydroxides, N-poor nitrides, metals or hydrides. To complete the chemical loop, the N-rich nitrides and imides need to be regenerated. In this section, we summarize and analyze the reaction thermodynamics of ammonia production from metal nitrides, including main group metals and transition metals, and metal imides, as well as the regeneration reaction thermodynamics of metal nitrides and imides.

3.1 The reaction thermodynamics of main group metal nitrides

The main group metals include s- and p-block elements. There are a large number of main group metal nitrides. Here, we select Li, Be, Mg, Ca, Sr, Ba, and Al as representatives to analyze their reaction thermodynamics. All of the reaction equations about the main group metal nitrides-mediated CLAS are listed in Table S1, and the thermodynamic calculation results are shown in Fig. 2.

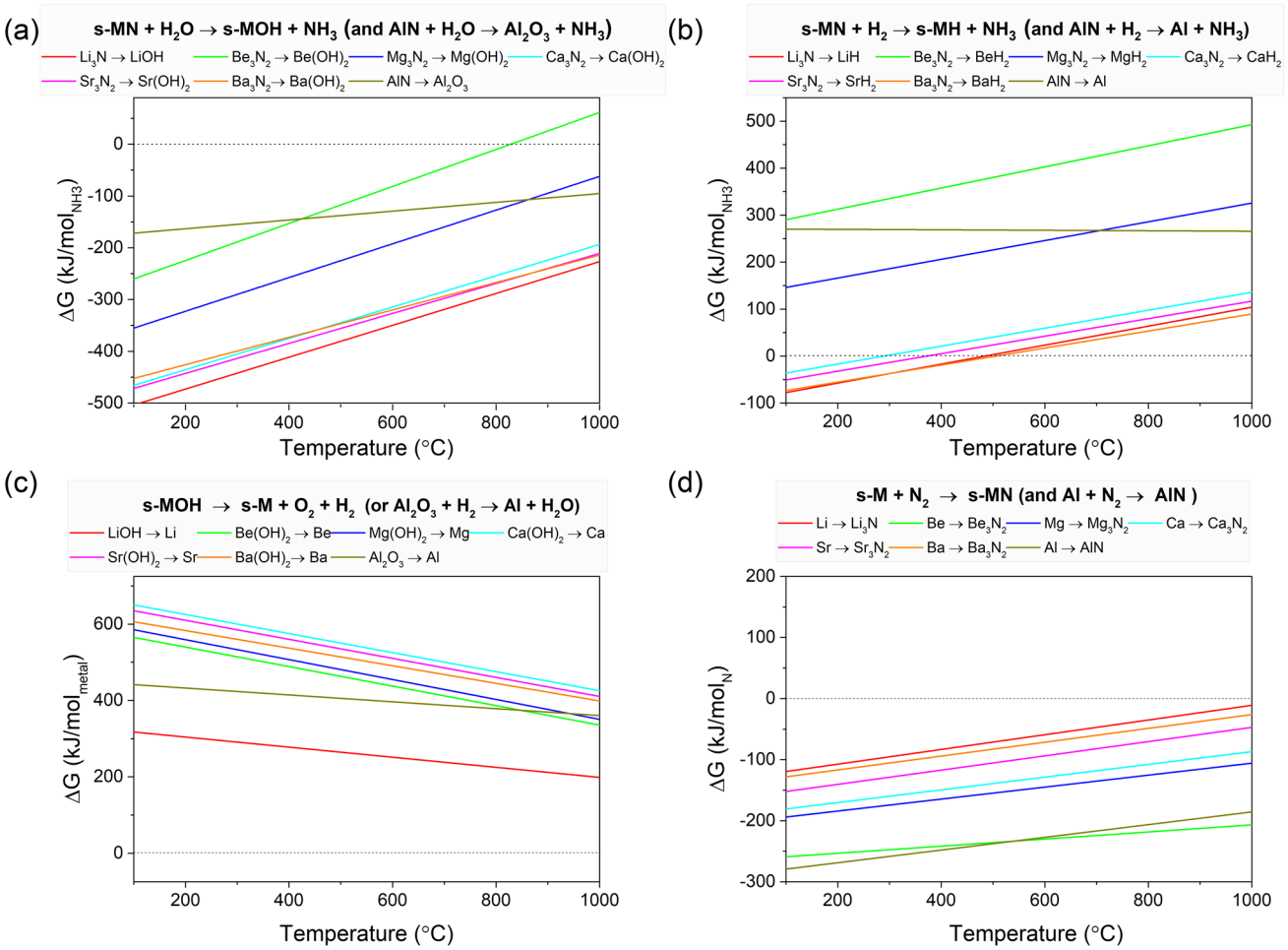

Fig. 2 The reaction chemistries of main group metal nitrides (s-MNs and p-MNs) for CLAS. **a**. The Gibbs free energy of s-MNs and p-MNs hydrolysis to produce ammonia as a function of temperature. **b**. The Gibbs free energy of s-MNs and p-MNs hydrogenation to produce ammonia as a function of temperature. **c**. The Gibbs free energy of main group metal hydroxides (or oxides) decomposition or reduction to generate the corresponding metals as a function of temperature. **d**. The Gibbs free energy of main group metal nitridation to generate corresponding metal nitrides as a function of temperature. The calculation of Gibbs free energy is based on the equation of $\Delta G = \Delta H - T\Delta S$ according to the reaction equations listed in Table S1, in which the standard formation enthalpy and standard entropy data of the reactants and products are taken from ref. [121, 122]

Figure 2a shows the reaction thermodynamics of s-MNs and p-MNs hydrolysis. It is seen that the Gibbs free energies of the hydrolysis reactions for all s-MNs are negative below 800 °C, suggesting these reactions spontaneously occur from the viewpoint of thermodynamics. The hydrolysis of alkali and alkaline earth metal nitrides to generate NH_3 and corresponding alkali and alkaline earth metal hydroxides (s-MOHs) can take place at low temperatures. The hydrolysis of aluminum nitride (AlN) requires high-temperature conditions due to large kinetic barriers, although it is thermodynamically favorable in the temperature range in Fig. 2a. The product of AlN hydrolysis is aluminum oxide (Al_2O_3) rather than aluminum hydroxide ($Al(OH)_3$) at high temperatures [27]. Figure 2b shows the reaction thermodynamics of the hydrogenation of s-MNs and p-MNs to alkali and alkaline earth metal hydrides (s-MHs) and metallic aluminum (Al). We could obtain the following conclusions: (i). The order of thermodynamic feasibility is $Li_3N \approx Ba_3N_2 > Sr_3N_2 > Ca_3N_2 > Mg_3N_2 > AlN > Be_3N_2$; (ii). The thermodynamics of these reactions are more favorable at lower temperatures; (iii). The hydrogenation of Li_3N, Ba_3N_2, Sr_3N_2, and Ca_3N_2 to corresponding hydrides can spontaneously occur below 484 °C, 505 °C, 372 °C, and 289 °C, respectively (at the equilibrium constant (K) = 1).

There are generally two approaches to regenerating s-MNs from s-MOHs, i. e., (i) AOHs decompose to form metals, which are subject to nitrogen fixation to return to s-MNs; (ii) the hydrogenation of s-MOHs generates s-MHs, and the s-MHs then fix nitrogen to generate s-MNs. However, the N_2 fixation on s-MHs usually generates s-MNHs rather than s-MNs at relatively low-temperature conditions, which had been experimentally observed. We only discuss the former pathway

here, and the N_2 fixation on s-MHs will be discussed in the next section. For Al_2O_3, we consider the following pathway to regenerate the N carrier: hydrogenation of Al_2O_3 to Al (AlH_3 is unstable), and Al then fixes nitrogen to generate AlN. Figure 2c shows the reaction thermodynamics of s-MOHs decomposition to alkali and alkaline earth metal as well as the hydrogenation of Al_2O_3 to generate Al. It is seen that all of these reactions are thermodynamically unfavorable in the shown temperature range. These highly endothermic reactions could be carried out using concentrated solar energy as the source of heat energy. Alternatively, the introduction of extrinsic stimuli such as electricity, photon, etc. is another promising and green method to make a thermodynamically unfavorable reaction occur under lower temperatures [32, 52], which will be discussed in the next section.

Figure 2d shows the reaction thermodynamics of N_2 fixation on alkali and alkaline earth metals as well as Al to generate s-MNs and AlN. It is seen that the reactions of N_2 fixation on these metals spontaneously occur from the viewpoint of thermodynamics, and the lower temperature is more favorable for these reactions.

In summary, the H_2O-CLAS processes over s-MNs should overcome the thermodynamic barriers of the decomposition of s-MOHs to generate alkali and alkaline earth metals. Moreover, in the H_2-CLAS over s-MNs, the N carrier will change from nitrides to imides. For the AlN-mediated H_2O-CLAS, it is limited by the step of Al_2O_3 reduction to Al. Furthermore, the hydrogenation of AlN to produce NH_3 is the thermodynamically determining step for AlN-mediated H_2-CLAS.

3.2 The reaction thermodynamics of transition metal nitrides and rare earth metal nitrides

Transition metals (TMs) and rare earth metals (REs) contain d- or f-block valence electrons with versatile physical and chemical properties, and their nitrides are abundant [53–56]. In this section, we will discuss several transition metal nitrides (TMNs) including Ti, V, Cr, Mn, Fe, Co, and Zn as well as two rare earth metals nitrides (LaN and YN) (RENs). These nitrides could react with H_2O to produce NH_3 and corresponding oxides (TMOs or REOs) [44, 49, 57]. In addition, they could also react with H_2 to produce NH_3 and generate the N-poor carriers, i.e., metals, N-poor TMNs [30], transition metal hydrides (TMHs) [58], or rare earth metal hydrides (REHs) [59].

To achieve an H_2O-CLAS over TMNs and RENs, TMOs or REOs should be regenerated to the corresponding nitrides. TMOs and REOs should be first reduced to corresponding metals or metal hydrides. For the oxides of V, Cr, Mn, Fe, Co, and Zn, they could be reduced to the corresponding metals by H_2. For the elements of La, Y, and Ti, their hydrides are usually more stable than their metallic states in the H_2 atmosphere, so we assume that the oxides of these three metals would be reduced to corresponding metal hydrides by H_2 [58, 59]. Then, these metals and metal hydrides could fix N_2 to form corresponding metal nitrides so as to close the H_2O-CLAS loop. On the other hand, to achieve an H_2-CLAS over TMNs and RENs, the N-poor carriers should be nitridized to metal nitrides. In this section, we calculate the reaction thermodynamics of TMNs and RENs reacting with H_2O and H_2 to produce NH_3, reduction of TMOs and REOs to form the N-poor carriers, and the N_2 fixation on these N-poor carriers to generate TMNs and RENs. All of the reaction equations about TMNs and RENs-mediated CLAS are listed in Table S2, and the thermodynamic calculation results are shown in Fig. 3.

Figure 3a shows the reaction thermodynamics of the nitrides reacting with H_2O to produce NH_3 and corresponding oxides. It can be seen that all of these reactions could occur in the shown temperature range and low T is more favorable from the viewpoint of thermodynamics. The order of thermodynamic feasibility is YN > LaN ≈ Cr_2N > Mn_4N > Zn_3N_2 > Mn_5N_2 > TiN > VN > Fe_4N > Co_3N.

Figure. 3b shows the reaction thermodynamics of the hydrogenations of these nitrides to produce NH_3 and generate corresponding N-poor carriers. It can be seen that the hydrogenations of Zn_3N_2, Fe_4N, and Co_3N are thermodynamically feasible below 400 °C for Fe and the whole shown temperature range for Zn and Co (at K = 1). Moreover, the hydrogenations of N-rich CrN and Mn_5N_2 to N-poor Cr_2N and Mn_4N could occur under high H_2 pressure and low NH_3 concentration conditions and the other reactions are more thermodynamically difficult considering the value of Gibbs free energy.

Figure. 3c shows the reaction thermodynamics of the regeneration of these nitrides from their oxides. The results show that the reduction of the late transition metal oxides (Fe_2O_3 and CoO) to corresponding metals is thermodynamically feasible, but the reduction of the other metal oxides is thermodynamically unfavorable.

Figure. 3d shows the reaction thermodynamics of N_2 fixation on TMs, N-poor TMs, and metal hydrides to generate corresponding metal nitrides. It can be seen that the nitridation of the TMs (V, Cr, and Mn), TMHs (TiH_2), N-poor TMNs (Cr_2N, Mn_4N), and REHs (LaH_2, YH_3) is thermodynamically feasible. However, the nitridation of Fe, Co, and Zn is thermodynamically unfavorable. The synthesis of Fe_4N, Co_3N, and Zn_3N_2 is usually via the nitridation reaction of metal or oxide powders in an NH_3 atmosphere [60–62].

The above thermodynamic calculation results indicate that the reduction of metal oxides of early transition metal (Ti, V, Cr, and Mn) and rare-earth metal (Y and La) and the N_2 fixation on late transition metals (Fe, Co, and Zn) are the

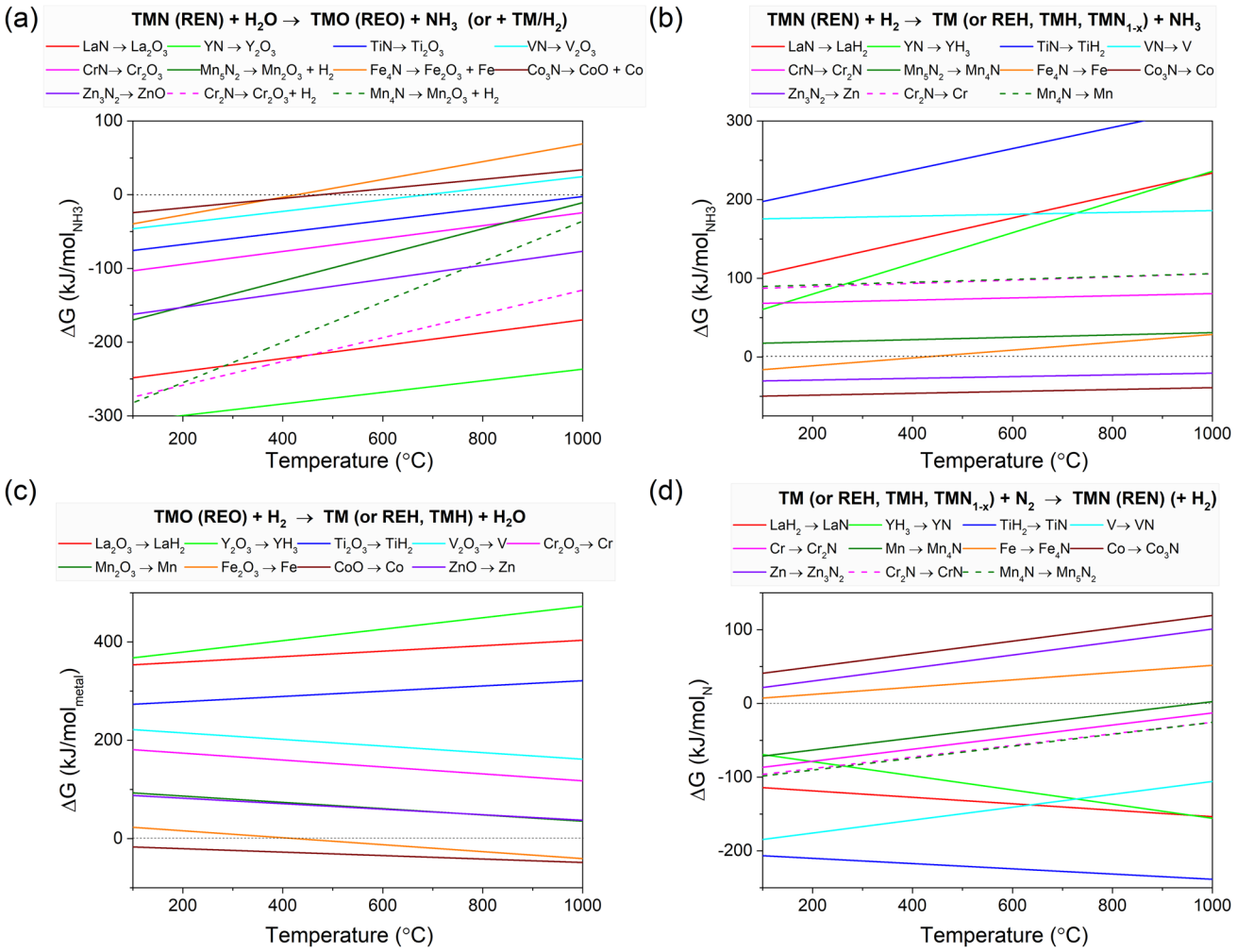

Fig. 3 The reaction chemistries of TMNs and RENs for CLAS. **a**. The Gibbs free energy of TMNs and RENs hydrolysis to produce ammonia as a function of temperature. **b**. The Gibbs free energy of TMNs and RENs hydrogenation to produce ammonia as a function of temperature. **c**. The Gibbs free energy of TMOs and REOs hydrogenation to generate metals as a function of temperature. **d**. The Gibbs free energy of metals (or metal hydrides) to generate corresponding nitrides as a function of temperature. The Gibbs free energy is calculated according to the reaction equations listed in Table S2 and the thermodynamic data of the reactants and products are taken from ref. [121, 122]

thermodynamic limiting steps in the TMNs and RENs-mediated H_2O-CLAS, respectively. In addition, the hydrogenations of early TMNs and RENs and N_2 fixation on late transition metals are the thermodynamic limiting steps in the TMNs and RENs-mediated H_2-CLAS.

3.3 The reaction thermodynamics of metal imides

Metal imides include s-MNHs [41, 63, 64], rare earth metals binary imides (RENHs) [65], ternary mixed cation imides [42, 66], ternary mixed anion imides [67, 68], etc. Due to the lack of thermodynamic data for most metal imides, we only discuss a portion of binary s-MNHs for application in the CLAS. s-MNHs can react with H_2 or H_2O to produce NH_3 and generate s-MHs or s-MOHs, respectively. The decomposition of s-MOHs to metals, which is thermodynamically unfavorable, is discussed in the Sect. 3.1 [31]. Here, we discuss the s-MNHs-mediated H_2-CLAS, which contains two steps: (i) hydrogenation of s-MNHs to produce NH_3 and generate s-MHs, and (ii) N_2 fixation on s-MH to generate s-MNH accompanied by H_2 release [34]. All of the reaction equations about ANHs-mediated CLAS are listed in Table S3, and the thermodynamic calculation results are shown in Fig. 4.

Figure 4a shows the reaction thermodynamics of s-MNHs hydrogenation to produce NH_3 and generate s-MHs. The results suggest that there is a low equilibrium concentration for the reaction of ANHs hydrogenation due to the positive

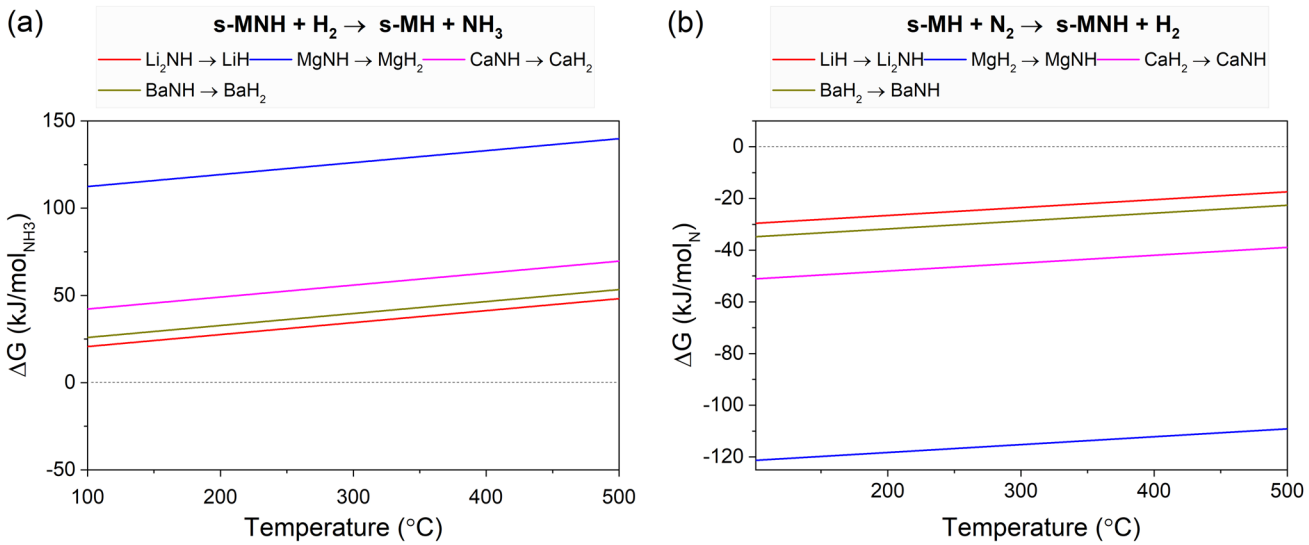

Fig. 4 The reaction chemistries of alkali and alkaline earth metal imides for CLAS. **a**. The Gibbs free energy of metal imides hydrogenation to produce ammonia as a function of temperature. **b**. The Gibbs free energy of metal hydrides nitridation to regeneration metal imides as a function of temperature. The solid entropies are not considered in the thermodynamic calculations due to the lack of entropies data for metal imides. The Gibbs free energy is calculated according to the reaction equations listed in Table S2, and the thermodynamic data of the reactants and products are taken from ref. [121, 122] and the entropy of solids is not considered in the calculation of Gibbs free energy

Gibbs free energy and the low temperature is more thermodynamically favorable. Figure 4b shows the reaction thermodynamics of s-MHs nitridation to generate s-MNHs and H_2. The results show that the nitridation reactions of various s-MHs are thermodynamically feasible. Considering the thermodynamics of these two steps, the order of thermodynamic feasibility of s-MNHs in the H_2-CLAS is BaNH ≈ Li_2NH > CaNH > MgNH [34]. It should be mentioned that the CaNH and MgNH could decompose or (de)hydrogenated to Ca_2NH (or Ca_3N_2) [69–71] and Mg_3N_2 [71, 72], respectively, at the certain conditions, which would form new loops for CLAS.

Compared to metal nitrides-mediated H_2O-CLAS and H_2-CLAS, the metal imides-mediated H_2-CLAS processes possess higher ammonia production rates and can be operated under milder reaction conditions as the literature reported [34]. However, the imides N carriers were less explored, and lack of thermodynamic data for these materials up to now. There is huge space to explore new imides materials, such as rare earth metals imides, and ternary imides, for application in the CLAS [73].

3.4 The thermodynamic improvement for the N carriers

An ideal N carrier material should possess suitable thermodynamic properties for each sub-reaction in the CLAS process. However, few materials can meet this requirement. For one thing, the development of new nitrides or imides materials should be encouraged. For another thing, the following strategies can be considered to improve the thermodynamic properties of N carriers. (i). Doping. The dopants can modify the chemical composition of N carriers and the bond strength of M–N, which would influence the thermodynamics of materials. Hargreaves et al. studied the role of lithium dopant in manganese nitride by combining theoretical and in-situ experimental investigations [74]. They found that the lithium dopant modifies the bulk and surface structure of manganese nitride and enhances hydrogen activation. Liu et al. studied the transition metal heteroatoms (Cr, Fe, Co, Ni, Mo) doped Mn_4N and Mn_2N lattices by DFT calculations [75]. They found that the dopant influences the covalency of metal-N bonding. (2). Compositing. The chemical reactions taking place in composite N carrier systems could be different from those in the single N carrier, which could form a new reaction pathway. Guo and Cao et al. developed multi-functional composite nitrogen carriers Li_2NH-Mn_2N and BaNH-Mn_2N for CLAS [51]. In these composite nitrogen carrier systems, the reaction of nitride N carrier with hydride to form the N-poor carrier (and imide), are more thermodynamically favorable than those reactions of nitride N carrier with hydrogen to form the N-poor carrier (and NH_3), and NH_3 production could follow the below reactions: (i) $AH + Mn_2N \rightarrow ANH + Mn_4N + H_2$; (ii)$ANH + H_2 \rightarrow AH + NH_3$. (3). Forming high-entropy compounds. High-entropy compounds have unique structures with the coexistence of antisite disordering and crystal periodicity,

which provide opportunities for various applications [76–78]. Some high-entropy oxides have been applied in the chemical looping process, which provided outstanding performance for thermochemical water splitting [79, 80]. We believe that there are potential promising chances to explore high-entropy nitrides or imides materials for CLAS [81, 82]. It should be mentioned that these strategies not only improve the thermodynamic properties of N carriers but also could enhance the kinetics performance of CLAS.

With the development of computational theories and the improvement of calculation speed, theoretical calculation and artificial intelligence (AI) have become effective means to assist material design [83–86]. They can be used to assist in the screening and design of N carriers with suitable thermodynamic properties. Michalsky et al. used the method of computational screening to search for suitable perovskite redox materials for H_2O-CLAS [87]. Musgrave and Holder et al. used the method of high-throughput equilibrium analysis to screen 1,148 metal nitride/metal oxide pairs for CLAS based on calculated Gibbs energies of these materials acquired from the Materials Project (MP) database [88]. Yang et al. investigated 1699 bicationic inorganic redox pairs for CLAS by high-throughput screening based on MP database [89]. It can be expected that theoretical calculation and AI will play a more important role in CLAS in the future.

4 Electricity-driven CLAS

Based on the above thermodynamic analysis, it can be seen that the performances of s-MNs, early TMNs, and RENs in the H_2O-CLAS processes are limited by the conversion of s-MOHs to metal [31], the reduction of TMOs to TMs (or TMHs), and the reduction of REOs to REHs, respectively [44, 57]. The performances of late TMNs in the H_2O-CLAS processes are limited by the nitridation of TMs to generate TMNs [90]. Electrification provides a pathway to break the thermal equilibrium limit of a reaction, which can be used to address the difficult step in the chemical looping process [31]. Such as water splitting to produce hydrogen and reduction of carbon dioxide to produce chemicals are the extremely thermodynamically unfavorable reactions, however, they can be carried out efficiently under electrically driven conditions [91, 92]. In addition, building electrochemical processes can contribute to achieving the storage and utilization of renewable energy and reducing carbon emissions [93, 94]. Here, we list several electrochemical

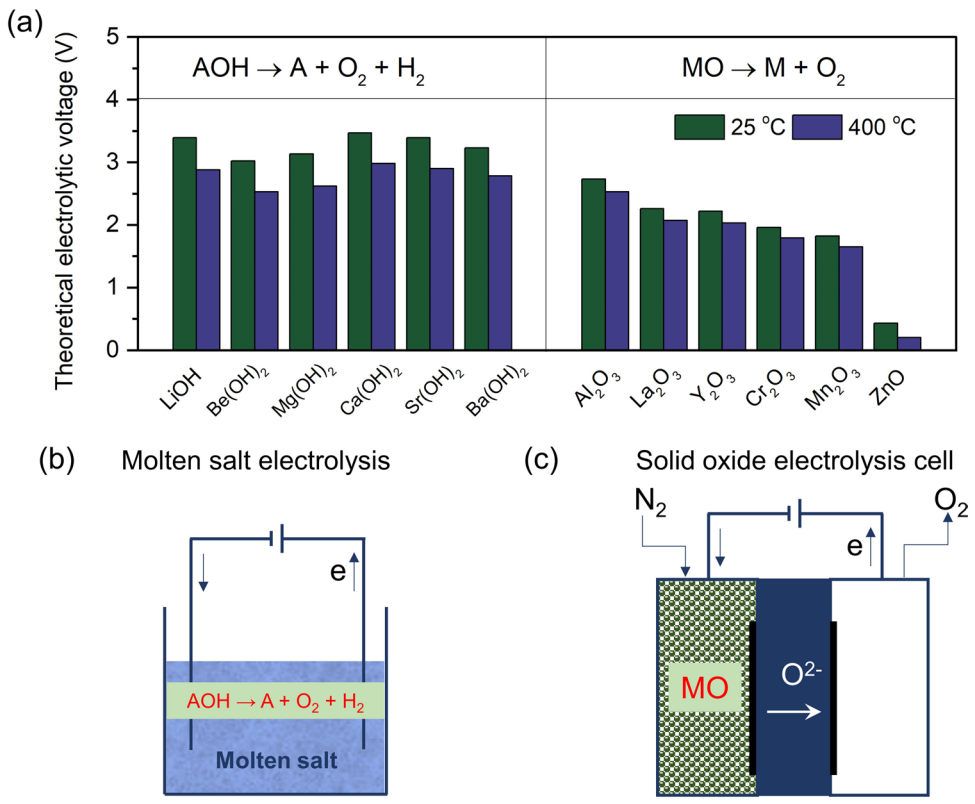

Fig. 5 Electrochemistry for the regeneration of N carriers. **a**. Theoretically electrolytic voltage of metal hydroxides decomposition to metals, metal oxides decomposition to metals, metal imides hydrogenation to metal hydrides. **b**, **c**. Schematic diagram of electrolytic cell based on molten salt electrolyte **b**, solid oxide ion conductor **c**

processes to achieve the CLAS process based on various N carriers. Figure 5a shows the theoretical voltage of some chemical sub-reactions at 25 °C and 400 °C. Figure 5b and c show the schematic diagrams of some electrolytic cells.

4.1 Electrolysis of s-MOHs to produce metal

As above mentioned, the industrial production of alkali and alkaline earth metals is using the method of electrolysis of their chlorides. Nørskov and Jaramillo et al. had proposed the electrolysis of LiOH to produce Li and proposed a Li_3N-LiOH-Li-mediated H_2O-CLAS [31]. In their work, the controlled molten salt mixture LiOH-LiCl was used as electrolyze to electrolysis of LiOH based on a molten salt electrolytic cell at cell potential minimum of 3.0 V and 450 °C. Similar to this process, the electrolysis of s-MOHs to produce corresponding metals can be used to construct s-MNs-mediated H_2O-CLAS processes. Figure 5a shows the thermodynamically electrolytic voltage of s-MOHs to metals at 25 °C and 400 °C. The values of all s-MOHs are in-between 2.5 V to 3.5 V. Alkali and alkaline earth metals can be produced in the molten salt system as shown in Fig. 5b. Besides, some Li (or Na, K, Mg, Al, etc.) battery devices could be used to produce corresponding metals [95, 96]. In future, the low-temperature molten salt or ion liquid could be used as electrolyte to reduce the reaction temperature, and efficient electrode material should be developed to reduce operating voltage.

4.2 Electro-reduction of metal oxide to metal

The thermal reduction of early TMOs and REOs to metals or metal hydrides is thermodynamically unfavorable from the above thermodynamic analysis (Fig. 3c). However, the theoretical electrolytic voltages of various metal oxides are below 3.0 V (Fig. 5a). The order of voltage value for various metal oxides is $Al_2O_3 > La_2O_3 > Y_2O_3 > Cr_2O_3 > Mn_2O_3 > ZnO$, which decreases with the increase in temperature. Moreover, the theoretical electrolytic voltage of Zn is only 0.2 V at 400 °C. Fray et al. found a solid metal oxide can be directly reduced to metal based on a molten salt electrolytic cell [97]. Subsequently, this sample method was widely used to produce various metals or alloys [98]. Besides, solid oxide oxygen-ion-conductors were used as electrolyte to produce various metals, such as Mg, Al, Ti, Ca, Fe, Cu, Ta, Cr, Ce. This process has advantages such as simplified design, lower cost, lower energy use, and zero emissions [99]. Recently, the technologies of solid oxide fuel cell (SOFC) and solid oxide electrolysis cell (SOEC) have made great progress in the development of electrolytic devices, electrolyte materials, electrocatalysts, and fabrication technology [100–105]. Here, we put forward to reduce metal oxide to produce metal by a SOEC device. Figure 5c shows the schematic diagram of a SOEC for the electrolysis of MOs. It will be important to develop a low-temperature O ion conductor and efficient electrocatalyst and optimize the electrode–electrolyte interface to achieve this process.

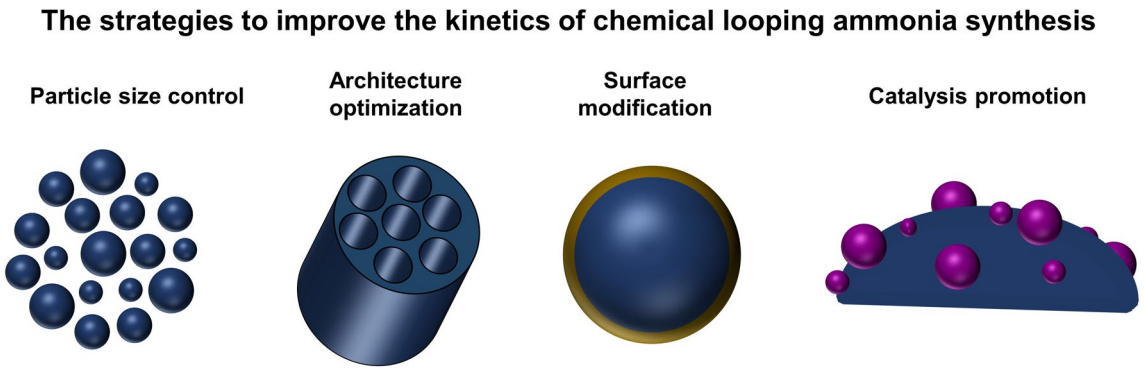

Fig. 6 Schematic diagram of kinetic improvement for CLAS

5 Kinetics improvement for CLAS

Beyond the thermodynamic property of N carriers, the kinetic property of N carriers is another key issue for the CLAS processes. Plenty of research have been performed to investigate the kinetics of chemical looping reactions. The following strategies have been generally used and demonstrated to be feasible for the kinetic improvement (Fig. 6).

5.1 Particle size control

In general, reducing the particle size could increase the reactivity of the materials, which have been used to improve the performance of O carrier materials [106]. Cwiertny and Grassian et al. investigated the particle size effects of α-Fe_2O_3 nanoparticles as oxygen carriers for chemical looping methane combustion. They found that decreasing particle size of α-Fe_2O_3 (from 350 to 3 nm) could increase the duration of CH_4 was completely converted to CO_2 due to smaller particles with higher surface area-to-volume ratios. Reduction and reoxidation cycling experiments showed that the efficiency of large particle sample (350 nm) reduced fast in the first three cycle and remained stable subsequently. However, the efficiency of small particle sample (50 nm and 3 nm) was continuous declination [107]. For the CLAS, our previous work showed that the NH_3 production rate was significantly enhanced when BaNH was dispersed on a large specific surface area Al_2O_3 support, which could increase the number of reactive sites [34]. Similarly, Shen et al. reported that the N-sorption capability of Mn-/Fe-based nitrogen carriers can be improved by loading the N carrier on the Al_2O_3 support [108]. Miyaoka et al. reported that the addition of Li_2O into LiH can prevent the agglomeration of the products and thus improve the kinetics of Li_2NH-LiH mediated H_2-CLAS [109]. On the other hand, it had been found that N_2 activation is sensitive to the structure of active sites, for example, B5 site for Ru-based and C7 site for Fe-based in catalytic ammonia synthesis, and size-control could adjust the surface structure of catalysts and influence the number of active sites [110, 111].

5.2 Architecture optimization

The architecture of N carriers and support could affect the transport and diffusion of reactants and products. It has been reported that the core–shell architecture of O carriers and support could increase the activity and selectivity of a chemical looping process [112, 113]. For example, Li et al. synthesized a Fe_2O_3@$La_{0.8}Sr_{0.2}FeO_{3-\delta}$ (LSF) core–shell redox catalyst used in CH_4 partial oxidation reaction [113]. In this structure, iron oxide core serves as the primary source of lattice-oxygen and LSF shell provides an active surface and facilitates O^{2-} and electron conductions. Besides, the inert LSF shell could enhance the selectivity of syngas by reducing the reactivity of lattice oxygen to prevent complete oxidation of CH_4, and improve stability of the primary oxide Fe_2O_3 by preventing particles from aggregating. AlN is one of the most studied N carriers for CLAS. It was found that the pore structure and specific surface area of AlN have a great effect on its ammonia production performance. Zhang et al. [114] synthesized a supported Al-based nitrogen carrier (AlN/Al_2O_3) with a mesoporous structure by the carbothermal reduction method. They found that the excess Al_2O_3 led to the significant improvement in N-carrier's porosity and thus ammonia production reactivity. With the technological development of the controllable synthesis of materials, the rational design and precise control of new structures could potentially improve the performance of N carriers.

5.3 Surface modification

A chemical looping reaction is composed of the following several steps, i.e., the adsorption and activation of reactants on the surface, the diffusion of ions in the bulk phase, and the desorption of products. The surface properties of N carriers are important for their reactivity. The hydrolysis of AlN is thermodynamically feasible at low temperatures, but suffers from a large kinetic energy barrier. With the aid of DFT calculations, Bartel et al. proposed that the hydrolysis of AlN, including water adsorption, hydroxyl-mediated proton diffusion to form NH_3, and NH_3 desorption, is enabled by the diffusion of protons across the AlN surface by a hydroxyl-mediated Grotthuss mechanism [115]. This work suggested that the surface properties can have a great influence on the reactivity of N carriers, which could be helpful to guide material design.. Moreover, a lot of research found that the surface modifications of O carriers could improve their activity and selectivity [116, 117]. Li et al. [116] employed alkali metal (Li, Na, and/or K)-promoted

$La_xSr_{2-x}FeO_{4-\delta}$ as redox catalysts for chemical looping oxidative dehydrogenation of ethane. They found that the surface layer of alkali metal oxide on the surface of catalysts increased the resistance for O^{2-} diffusion from the bulk and its subsequent evolution into electrophilic oxygen species on the surface, so the nonselective oxidation of ethane is inhibited. In another work, they found that promoting mixed oxides with a small amount of Rh can lower the onset temperature of methane partial oxidation by as much as 300 °C [117]. It was suggested that Rh on the surface could enhance methane C–H bond activation, which leads to higher concentrations of surface CH_x species for facile oxygen extraction from the surface. These surface modification methods in the design of O carriers may be helpful for the design of N carrier materials.

5.4 Catalysis promotion

One of the most common means to accelerate the rate of a reaction is via adding catalysts. Many works have shown that catalysts could enhance the performance of CLAS. Wu et al. found that Fe_2O_3 and TiO_2 could catalyze the N-desorption step of AlN in a H_2O-CLAS [48, 118]. Liu et al. found TM doping (Cr, Fe, Co, Ni, Mo) or loading (Fe_3 and Ni_3 clusters) on manganese nitrides could facilitate ammonia synthesis by manipulating the geometric and electronic structures based on DFT calculations [75, 119]. Shen et al. found that there is a synergistic effect of Mn- and Fe-based nitrogen carriers for CLAS. In this process, one N carrier could catalyze the chemical looping reactions of the other N carrier [120]. Laassiri et al. found the lithium dopant in manganese nitride could enhance the manganese nitride for H_2-CLAS [74]. As mentioned before, doping also changes the thermodynamic property of N carriers. Moreover, our recent works have shown that TM and TMN catalysts could catalyze the N_2 fixation on AH and hydrogenation of ANH in the ANH-mediated H_2-CLAS [34, 51]. Except for the above strategies, external-field assistance, composition optimization, etc. could also be used to improve the kinetics.

As mentioned in Sect. 4, an electricity-driven approach provides an alternative route to make those thermodynamically unfavorable reactions occur at low theoretical potentials. However, the kinetic behaviors in this process such as gas/solid phase mass transfer, charge transfer, and gas–solid interfacial reaction etc. should be also considered. The above-mentioned strategies for kinetics improvement can also be used in the electrochemical reactions. For example, we can control the size and architecture of N carrier materials as well as catalysts to enhance the gas/ions transfer in the pore and bulk, respectively. The surface modification could influence the charge transfer and surface reaction processes. Besides, active electrode materials are demanded to efficiently catalyze the electrode reactions and reduce the overpotentials. More studies are needed on this aspect to fulfill the promising electro-driven CLAS process.

6 Conclusion

Chemical looping ammonia synthesis is a promising research field due to the advantages in breaking scaling relations and avoiding competitive adsorption. The development of efficient N carriers is vital for this process. This paper summarized the reaction thermodynamics of H_2-CLAS and H_2O-CLAS based on N carriers of main group metal and transition metal nitrides, and metal imides. The thermodynamically limited steps, for example, the reduction of metal hydroxides/oxides to metals or metal hydrides, the hydrogenation of metal nitrides/imides, could be improved by the electricity-driven method. Moreover, the strategies for improving the chemical looping reaction kinetics were summarized, in which the controllable synthesis of N carriers and the development of efficient catalysts could be important research directions. In future, high throughput synthesis and artificial intelligence may be helpful for the screening of N carriers, and the engineering design of the reactor and operation process should be developed for practical application.

Acknowledgements The authors acknowledge the Projects supported by the National Key R&D Program of China (2021YFB4000400), the National Natural Science Foundation of China (22109158, 22279131, and 21988101), the Youth Innovation Promotion Association CAS (2022180), the LiaoNing Revitalization Talents Program (XLYC2002076, XLYC2007173).

Author contributions PC and JG conceived the project. WG wrote the manuscript. RW, SF, YW, ZS checked the thermodynamics data used in the manuscript. PC and JG revised the manuscript. All authors read and approved the final manuscript.

Data availability All data are available on reasonable request.

Declarations

Competing interests The authors declare no competing interests.

References

1. Valera-Medina A, Xiao H, Owen-Jones M. Ammonia for power. Prog Energy Combust Sci. 2018. https://doi.org/10.1016/j.pecs.2018.07.001.
2. Chang F, Gao W, Guo J. Emerging materials and methods toward ammonia-based energy storage and conversion. Adv Mater. 2021;50:2005721.
3. Guo J, Chen P. Catalyst: NH_3 as an energy carrier. Chem. 2017;5:709–12.
4. Chen JG, Crooks RM, Seefeldt LC. Beyond fossil fuel-driven nitrogen transformations. Science. 2018. https://doi.org/10.1126/science.aar6611.
5. Smith C, Hill AK, Torrente-Murciano L. Current and future role of Haber-Bosch ammonia in a carbon-free energy landscape. Energ Environ Sci. 2020;2:331–44.
6. Lai Q, Cai T, Tsang SCE. Chemical looping based ammonia production—A promising pathway for production of the noncarbon fuel. Sci Bull. 2022;20:2124–38.
7. Zhang S, Zhao Y, Shi R. Photocatalytic ammonia synthesis: Recent progress and future. EnergyChem. 2019;2:100013.
8. Marakatti VS, Gaigneaux EM. Recent advances in heterogeneous catalysis for ammonia synthesis. ChemCatChem. 2020;23:5838–57.
9. Qing G, Ghazfar R, Jackowski ST. Recent advances and challenges of electrocatalytic N_2 reduction to ammonia. Chem Rev. 2020;12:5437–516.
10. Kong Y, Li Y, Sang X. Atomically dispersed zinc(I) active sites to accelerate nitrogen reduction kinetics for ammonia electrosynthesis. Adv Mater. 2021. https://doi.org/10.1002/adma.202103548.
11. Yuan Y, Zhou L, Robatjazi H. Earth-abundant photocatalyst for H_2 generation from NH_3 with light-emitting diode illumination. Science. 2022;6622:889–93.
12. Hajduk Š, Dasireddy VDBC, Likozar B, Dražić G, Orel ZC. COx-free hydrogen production via decomposition of ammonia over Cu–Zn-based heterogeneous catalysts and their activity/stability. Appl Catal B Environ. 2017;211:57–67.
13. Guo J, Wang P, Wu G. Lithium imide synergy with 3d transition-metal nitrides leading to unprecedented catalytic activities for ammonia decomposition. Angew Chem Int Ed Engl. 2015;10:2950–4.
14. Vojvodic A, Medford AJ, Studt F. Exploring the limits: a low-pressure, low-temperature haber-bosch process. Chem Phys Lett. 2014. https://doi.org/10.1016/j.cplett.2014.03.003.
15. Joshi A, Shah V, Mohapatra P. Chemical looping-A perspective on the next-gen technology for efficient fossil fuel utilization. Adv Appl Energy. 2021;3:100044.
16. Sheng F, Wenbo G, Hujun C. Advances in the chemical looping ammonia synthesis. Acta Chim Sinica. 2020;9:916–27.
17. Juangsa FB, Irhamna AR, Aziz M. Production of ammonia as potential hydrogen carrier: review on thermochemical and electrochemical processes. Int J Hydrogen Energ. 2021;27:14455–77.
18. Burrows L, Gao P-X, Bollas GM. Thermodynamic feasibility analysis of distributed chemical looping ammonia synthesis. Chem Eng J. 2021;426:131421.
19. Juangsa FB, Aziz M. Integrated system of thermochemical cycle of ammonia, nitrogen production, and power generation. Int J Hydrogen Energ. 2019;33:17525–34.
20. Fang J, Xiong CH, Feng MQ. Utilization of carbon-based energy as raw material instead of fuel with low CO_2 emissions: energy analyses and process integration of chemical looping ammonia generation. Appl Energ. 2022. https://doi.org/10.1016/j.apenergy.2022.118809.
21. Wang X, Su M, Zhao H. Process design and exergy cost analysis of a chemical looping ammonia generation system using AlN/Al_2O_3 as a nitrogen carrier. Energy. 2021. https://doi.org/10.1016/j.energy.2021.120767.
22. Jennings JR. Catalytic ammonia synthesis: fundamentals and practice. Berlin: Springer; 1991.
23. Haber F, Van OG. Formation of ammonia from the elements. Z Anorg Chem. 1905;1:341.
24. Frank AR. On the utilisation of the atmospheric nitrogen in the production of calcium cyanamide and its use in agriculture and chemistry. Trans Fara Soc. 1908. https://doi.org/10.1039/tf9080400099.
25. Wang L, Xia M, Wang H. Greening ammonia toward the solar ammonia refinery. Joule. 2018;6:1055–74.
26. Zhao Y, Gao W, Li S. Solar-versus thermal-driven catalysis for energy conversion. Joule. 2019;4:920–37.
27. Gálvez ME, Halmann M, Steinfeld A. Ammonia production via a two-step Al2O3/AlN thermochemical cycle Thermodynamic, environmental, and economic analyses. Ind Eng Chem Res. 2007;7:2042–6.
28. McKay D, Gregory DH, Hargreaves JSJ. Towards nitrogen transfer catalysis: reactive lattice nitrogen in cobalt molybdenum nitride. Chem Commun. 2007;29:3051–3.
29. Munter TR, Bligaard T, Christensen CH. BEP relations for N_2 dissociation over stepped transition metal and alloy surfaces. Phys Chem Chem Phys. 2008;34:5202–6.
30. Michalsky R, Avram AM, Peterson BA. Chemical looping of metal nitride catalysts: Low-pressure ammonia synthesis for eergy storage. Chem Sci. 2015;7:3965–74.

31. McEnaney JM, Singh AR, Schwalbe JA. Ammonia synthesis from N_2 and H_2O using a lithium cycling electrification strategy at atmospheric pressure. Energ Environ Sci. 2017;7:1621–30.
32. Swearer DF, Knowles NR, Eyeritt HO. Light-driven chemical looping for ammonia synthesis. ACS Energy Lett. 2019;7:1505–12.
33. Brown SW, Robinson B, Wang Y. Microwave heated chemical looping ammonia synthesis over Fe and CoMo particles. J Mater Chem A. 2022;29:15497–507.
34. Gao W, Guo J, Wang P. Production of ammonia via a chemical looping process based on metal imides as ntrogen carriers. Nat Energy. 2018;12:1067–75.
35. Shinzato K, Tagawa K, Tsunematsu K. Systematic study on nitrogen dissociation and ammonia synthesis by lithium and group 14 element alloys. ACS Appl Energy Mater. 2022;4:4765–73.
36. Yamaguchi T, Shinzato K, Yamamoto K. Pseudo catalytic ammonia synthesis by lithium–tin alloy. Int J Hydrogen Energ. 2020;11:6806–12.
37. Tang Z, Meng X, Shi Y. Lithium-based loop for ambient-pressure ammonia synthesis in a liquid alloy-salt catalytic system. Chemsuschem. 2021;21:4697–707.
38. Niewa R, DiSalvo F. Recent developments in nitride chemistry. Chem Mater. 1998;10:2733–52.
39. Kroll P, Eck B, Dronskowski R. First-principles studies of extended nitride materials. Adv Mater. 2000;4:307–10.
40. Miessler G L. Inorganic chemistry. Pearson Education India; 2008
41. Chen P, Xiong Z, Luo J. Interaction of hydrogen with metal nitrides and imides. Nature. 2002;6913:302–4.
42. Xiong Z, Wu G, Hu J. Ternary imides for hydrogen storage. Adv Mater. 2004;17:1522–5.
43. He T, Cao H, Chen P. The roles of alkali/alkaline earth metals in the materials design and development for hydrogen storage. Acc Mater Res. 2021;9:726–38.
44. Michalsky R, Pfromm PH. Chromium as reactant for solar thermochemical synthesis of ammonia from steam, nitrogen, and biomass at atmospheric pressure. Sol Energy. 2011;11:2642–54.
45. Mehta P, Barboun PM, Engelmann Y. Plasma-catalytic ammonia synthesis beyond the equilibrium limit. ACS Catal. 2020;12:6726–34.
46. Marnellos G, Stoukides M. Ammonia synthesis at atmospheric pressure. Science. 1998;5386:98–100.
47. Mohandas K. Direct electrochemical conversion of metal oxides to metal by molten salt electrolysis: a review. Min Proc Extr Met. 2013;4:195–212.
48. Wu Y, Jiang G, Zhang H. Fe_2O_3, a cost effective and environmentally friendly catalyst for the generation of NH_3 - a future fuel - using a new Al_2O_3-looping based technology. Chem Commun. 2017;77:10664–7.
49. Michalsky R, Parman BJ, Amanor-Boadu V. Solar thermochemical production of ammonia from water, air and sunlight: thermodynamic and economic analyses. Energy. 2012;1:251–60.
50. Michalsky R, Pfromm PH, Steinfeld A. Rational design of metal nitride redox materials for solar-driven ammonia synthesis. Interface Focus. 2015;3:20140084.
51. Feng S, Gao W, Wang Q. A multi-functional composite nitrogen carrier for ammonia production via a chemical looping route. J Mater Chem A. 2021;2:1039–47.
52. Soloveichik G. Electrochemical synthesis of ammonia as a potential alternative to the Haber-Bosch process. Nat Catal. 2019;5:377–80.
53. Toth L. Transition metal carbides and nitrides. Amsterdam: Elsevier; 2014.
54. Oyama ST. The chemistry of transition metal carbides and nitrides. Berlin: Springer; 1996.
55. Sclar N. Properties of rare-earth nitrides. J Appl Phys. 1964;5:1534–8.
56. Eyring L, Gschneidner KA, Lander G. Handbook on the physics and chemistry of rare earths. Berlin: Elsevier; 2022.
57. Yan H, Gao W, Cui J. Dinitrogen fixation mediated by lanthanum hydride. J Energy Chem. 2022. https://doi.org/10.1016/j.jechem.2022.04.011.
58. Gibb TR Jr, Kruschwitz HW Jr. The titanium—hydrogen system and titanium hydride. I. low-pressure studies. J Am Chem Soc. 1950;12:5365–9.
59. Korst WL, Warf JC. Rare earth-hydrogen systems. I. structural and thermodynamic properties. Inorg Chem. 2002;10:1719–26.
60. Bartłomiej W, Arabczyk W. Investigation of nitriding and reduction processes in a nanocrystalline iron–ammonia–hydrogen system at 350 °C. Phys Chem Chem Phys. 2015;31:20185–93.
61. Widenmeyer M, Shlyk L, Becker N. Synthesis of metastable Co4N, Co3N, Co2N, and CoO0. 74N0. 24 from a single azide precursor and intermediates in CoBr 2 ammonolysis. Eur J Inorg Chem. 2016;29:4792–801.
62. Zong F, Ma H, Xue C. Synthesis and thermal stability of Zn_3N_2 powder. Solid State Commun. 2004;8:521–5.
63. Ichikawa T, Leng H, Isobe S. Recent development on hydrogen storage properties in metal–N–H systems. J Power Sources. 2006;1:126–31.
64. Chen P, Xiong Z, Wu G. Metal–N–H systems for the hydrogen storage. Scripta Mater. 2007;10:817–22.
65. Imamura H, Kawasoe M, Imayoshi K. Preparation and some properties of nanostructural rare earth nitrides by using the reaction of hydrides with ammonia. Int J Theor Appl Nanotech. 2015. https://doi.org/10.11159/ijtan.2015.001.
66. Wu H. Structure of ternary imide $Li_2Ca(NH)_2$ and hydrogen storage mechanisms in amide–hydride system. J Am Chem Soc. 2008;20:6515–22.
67. David WI, Jones MO, Gregory DH. A mechanism for non-stoichiometry in the lithium amide/lithium imide hydrogen storage reaction. J Am Chem Soc. 2007;6:1594–601.
68. Silva GC, Yeamans CB, Weck PF. Synthesis and characterization of $Th_2N_2(NH)$ Isomorphous to Th_2N_3. Inorg Chem. 2012;5:3332–40.
69. Chon S, Sugisawa Y, Kobayashi S. Selective epitaxial growth of Ca_2NH and CaNH thin films by reactive magnetron sputtering under hydrogen partial pressure control. J Phys Chem Lett. 2022;43:10169–74.
70. Xiong Z, Chen P, Wu G. Investigations into the interaction between hydrogen and calcium nitride. J Mater Chem. 2003;7:1676–80.
71. Nakamori Y, Kitahara G, Orimo S. Synthesis and dehydriding studies of Mg–N–H systems. J Power Sources. 2004;1–2:309–12.
72. Leng HY, Ichikawa T, Hino S. Synthesis and decomposition reactions of metal amides in metal–N–H hydrogen storage system. J Power Sources. 2006;2:166–70.
73. Veser G. Taking the pressure off. Nat. Energy. 2018;12:1025–6.
74. Laassiri S, Zeinalipour-Yazdi CD, Catlow CRA. The potential of manganese nitride based materials as nitrogen transfer reagents for nitrogen chemical looping. Appl Catal B Environ. 2018;223:60–6.
75. Shan N, Huang C, Lee RT. Manipulating the geometric and electronic structures of manganese nitrides for ammonia synthesis. ChemCatChem. 2020;8:2233–44.

76. Oses C, Toher C, Curtarolo S. High-entropy ceramics. Nat Rev Mater. 2020;4:295–309.
77. George EP, Raabe D, Ritchie RO. High-entropy alloys. Nat Rev Mater. 2019;8:515–34.
78. Ye Y, Wang Q, Lu J. High-entropy alloy: Challenges and prospects. Mater Today. 2016;6:349–62.
79. Zhai S, Rojas J, Ahlborg N. The use of poly-cation oxides to lower the temperature of two-step thermochemical water splitting. Energ Environ Sci. 2018;8:2172–8.
80. Gao Y, Mao Y, Song Z. Efficient generation of hydrogen by two-step thermochemical cycles: Successive thermal reduction and water splitting reactions using equal-power microwave irradiation and a high entropy material. Appl Energy. 2020;279:115777
81. Jin T, Sang X, Unocic RR. Mechanochemical-assisted synthesis of high-entropy metal nitride via a soft urea strategy. Adv Mater. 2018;23:1707512.
82. Hsieh M-H, Tsai M-H, Shen W-J. Structure and properties of two Al–Cr–Nb–Si–Ti high-entropy nitride coatings. Surf Coat Tech. 2013. https://doi.org/10.1016/j.surfcoat.2013.01.036.
83. Seh ZW, Kibsgaard J, Dickens CF. Combining theory and experiment in electrocatalysis Insights into materials design. Science. 2017. https://doi.org/10.1126/science.aad4998.
84. Gubernatis J, Lookman T. Machine learning in materials design and discovery: Examples from the present and suggestions for the future. Phys Rev Mater. 2018;12:120301.
85. Himanen L, Geurts A, Foster AS. Data-driven materials science: status, challenges, and perspectives. Adv Sci. 2019;21:1900808.
86. Wang X, Gao Y, Krzystowczyk E. High-throughput oxygen chemical potential engineering of perovskite oxides for chemical looping applications. Energ Environ Sci. 2022;4:1512–28.
87. Michalsky R, Steinfeld A. Computational screening of perovskite redox materials for solar thermochemical ammonia synthesis from N_2 and H_2O. Catal Today. 2017. https://doi.org/10.1016/j.cattod.2016.09.023.
88. Bartel CJ, Rumptz JR, Weimer AW. High-throughput equilibrium analysis of active materials for solar thermochemical ammonia synthesis. ACS Appl Mater Interfaces. 2019;28:24850–8.
89. Fan J, Li W, Li S. High-throughput screening of bicationic redox materials for chemical looping ammonia synthesis. Adv Sci. 2022;27:e2202811.
90. Alexander AM, Hargreaves JSJ, Mitchell C. The reduction of various nitrides under hydrogen: Ni_3N, Cu_3N, Zn_3N_2 and Ta_3N_5. Top Catal. 2012;14–15:1046–53.
91. Nitopi S, Bertheussen E, Scott SB. Progress and perspectives of electrochemical CO_2 reduction on copper in aqueous electrolyte. Chem Rev. 2019;12:7610–72.
92. Zhu J, Hu L, Zhao P. Recent advances in electrocatalytic hydrogen evolution using nanoparticles. Chem Rev. 2019;2:851–918.
93. Tang C, Zheng Y, Jaroniec M. Electrocatalytic refinery for sustainable production of fuels and chemicals. Angew Chem Int Ed Engl. 2021;36:19572–90.
94. MacFarlane DR, Cherepanov PV, Choi J. A roadmap to the ammonia economy. Joule. 2020;6:1186–205.
95. Zuo W, Li R, Zhou C. Battery-supercapacitor hybrid devices: recent progress and future prospects. Adv Sci. 2017;7:1600539.
96. Pistoia G. 2008 Battery operated devices and systems. In: portable electronics to industrial products. Elsevier, Berlin
97. Chen GZ, Fray DJ, Farthing TW. Direct electrochemical reduction of titanium dioxide to titanium in molten calcium chloride. Nature. 2000;6802:361–4.
98. Mohandas K. Direct electrochemical conversion of metal oxides to metal by molten salt electrolysis: a review. Min Proc Ext Met C. 2013;4:195–212.
99. Guan X, Pal UB, Jiang Y. Clean metals production by solid oxide membrane electrolysis process. J Sustain Metall. 2016;2:152–66.
100. Bian W, Wu W, Wang B. Revitalizing interface in protonic ceramic cells by acid etch. Nature. 2022;7906:479–85.
101. Duan C, Kee RJ, Zhu H. Highly durable, coking and sulfur tolerant, fuel-flexible protonic ceramic fuel cells. Nature. 2018;7704:217–22.
102. Duan C, Tong J, Shang M. Readily processed protonic ceramic fuel cells with high performance at low temperatures. Science. 2015;6254:1321–6.
103. Zheng Y, Wang J, Yu B. A review of high temperature co-electrolysis of H_2O and CO_2 to produce sustainable fuels using solid oxide electrolysis cells (SOECs): advanced materials and technology. Chem Soc Rev. 2017;5:1427–63.
104. Gao Y, Nolan AM, Du P. Classical and emerging characterization techniques for investigation of ion transport mechanisms in crystalline fast ionic conductors. Chem Rev. 2020;13:5954–6008.
105. Duan CC, Huang JK, Sullivan N. Proton-conducting oxides for energy conversion and storage. Appl Phys Rev. 2020;1:011314.
106. Mishra A, Li F. Chemical looping at the nanoscale—challenges and opportunities. Curr Opin Chem Eng. 2018. https://doi.org/10.1016/j.coche.2018.05.001.
107. Alalwan HA, Mason SE, Grassian VH. α-Fe_2O_3 nanoparticles as oxygen carriers for chemical looping combustion: an integrated materials characterization approach to understanding oxygen carrier performance, reduction mechanism, and particle size effects. Energ Fuels. 2018;7:7959–70.
108. Wang B, Guo H, Yin X. N-sorption capability of Al_2O_3-supported Mn-/Fe-based nitrogen carriers during chemical looping ammonia synthesis technology. Energ Fuel. 2020. https://doi.org/10.1021/acs.energyfuels.0c01000.
109. Tagawa K, Gi H, Shinzato K. Improvement of kinetics of ammonia synthesis at ambient pressure by the chemical looping process of lithium hydride. J Phys Chem C. 2022;5:2403–9.
110. Somorjai GA, Materer N. Surface structures in ammonia synthesis. Top Catal. 1994;3:215–31.
111. Honkala K, Hellman A, Remediakis IN. Ammonia synthesis from first-principles calculations. Science. 2005;5709:555–8.
112. Neal L, Shafiefarhood A, Li F. Effect of core and shell compositions on MeO_x@$La_ySr_{1-y}FeO_3$ core–shell redox catalysts for chemical looping reforming of methane. Appl Energy. 2015. https://doi.org/10.1016/j.apenergy.2015.06.028.
113. Neal LM, Shafiefarhood A, Li F. Dynamic methane partial oxidation using a Fe_2O_3@$La_{0.8}Sr_{0.2}FeO_{3-\delta}$ core–shell redox catalyst in the absence of gaseous oxygen. ACS Catal. 2014;10:3560–9.
114. Zhang Q, Wu Y, Gao Y. High-performance mesoporous (AlN/Al_2O_3) for enhanced NH_3 yield during chemical looping ammonia generation technology. Int J Hydrogen Energ. 2020;16:9903–13.
115. Bartel CJ, Muhich CL, Weimer AW. Aluminum nitride hydrolysis enabled by hydroxyl-mediated surface proton hopping. ACS Appl Mater Interfaces. 2016;28:18550–9.

116. Gao Y, Haeri F, He F. Alkali metal-promoted $La_xSr_{2-x}FeO_{4-\delta}$ redox catalysts for chemical looping oxidative dehydrogenation of ethane. ACS Catal. 2018;3:1757–66.
117. Shafiefarhood A, Zhang J, Neal LM. Rh-promoted mixed oxides for "low-temperature" methane partial oxidation in the absence of gaseous oxidants. J Mater Chem A. 2017;23:11930–9.
118. Gao Y, Wu Y, Zhang Q. N-desorption or NH_3 generation of TiO_2-loaded Al-based nitrogen carrier during chemical looping ammonia generation technology. Int J Hydrogen Energ. 2018;34:16589–97.
119. Liu B, Manavi N, Deng H. Activation of N_2 on manganese nitride-supported Ni_3 and Fe_3 clusters and relevance to ammonia formation. J Phys Chem Lett. 2021;28:6535–42.
120. Wang B, Yin X, Wang P. Chemical looping ammonia synthesis at atmospheric pressure benefiting from synergistic effect of Mn- and Fe-based nitrogen carriers. Int J Hydrogen Energ. 2022. https://doi.org/10.1016/j.ijhydene.2022.10.132.
121. Binnewies M, Milke E. Thermochemical data of elements and compounds. Hoboken: Wiley Online Library; 2002.
122. Haynes WM, Lide DR, Bruno TJ. CRC handbook of chemistry and physics. Boca Raton: CRC Press; 2016.